Available online at www.sciencedirect.com

SCIENCE DIRECT

Virology 324 (2004) 387–399

VIROLOGY

www.elsevier.com/locate/yviro

Mapping the assembly pathway of Bluetongue virus scaffolding protein VP3

Alak Kanti Kar,[a] Mrinal Ghosh,[a] and Polly Roy[a,b,*]

[a] *Department of Medicine, University of Alabama at Birmingham, Birmingham, AL 35294, USA*

[b] *Department of Infectious and Tropical Diseases, London School of Hygiene and Tropical Medicine, London WC1E 7HT, UK*

Received 9 January 2004; returned to author for revision 31 March 2004; accepted 13 April 2004

Abstract

The structure of the Bluetongue virus (BTV) core and its outer layer VP7 has been solved by X-ray crystallography, but the assembly intermediates that lead to the inner scaffolding VP3 layer have not been defined. In this report, we addressed two key questions: (a) the role of VP3 amino terminus in core assembly and its interaction with the transcription complex (TC) components; and (b) the assembly intermediates involved in the construction of the VP3 shell. To do this, deletion mutants in the amino terminal and decamer–decamer interacting region of VP3 (ΔDD) were generated, expressed in insect cells using baculovirus expression systems, and their ability to assemble into core-like particles (CLPs) and to incorporate the components of TC were investigated. Deletion of the N-terminal 5 (Δ5N) or 10 (Δ10N) amino acids did not affect the ability to assemble into CLPs in the presence of VP7 although the cores assembled using the 10 residue mutant (Δ10N) deletion were very unstable. Removal of five residues also did not effect incorporation of the internal VP1 RNA polymerase and VP4 mRNA capping enzyme proteins of the TC. Removal of the VP3–VP3 interacting domain (ΔDD) led to failure to assemble into CLPs yet retained interaction with VP1 and VP4. In solution, purified ΔDD mutant protein readily multimerized into dimers, pentamers, and decamers, suggesting that these oligomers are the authentic assembly intermediates of the subcore. However, unlike wild-type VP3 protein, the dimerization domain-deleted assembly intermediates were found to have lost RNA binding ability. Our study emphasizes the requirement of the N-terminus of VP3 for binding and encapsidation of the TC components, and defines the role of the dimerization domain in subcore assembly and RNA binding.

Keywords: Bluetongue virus; VP3; Core-like particles

Introduction

The largest family of segmented, double-stranded (ds) RNA virus, the *Reoviridae*, constitutes viruses that infect hosts ranging from insects to plants and humans (Mertens, 1999). Electron cryo-microscopy (Cryo-EM) in conjunction with X-ray crystallography has provided structural details of several viruses belonging to the various genera of *Reoviridae* and revealed that these viruses possess capsids of a complex nature. Overall similar structural arrangements of inner capsids of these diverse range of viruses indicate high structural constrains in certain proteins with distinct features in others relating to evolutionary impacts including the wide host range and tissue tropism (Grimes et al., 1998; Hewat et al., 1992; Hill et al., 1999; Lu et al., 1998; Prasad et al., 1992, 1996; Reinisch et al., 2000; Shaw et al., 1996).

Bluetongue virus (BTV) is the prototype strain of Orbivirus genus within the *Reoviridae* family. BTV, the etiological agent of Bluetongue disease, is an economically important disease of live stock and is transmitted by blood feeding insect *Culicoides* vectors from infected to healthy animals (Mellor, 1990). Like other members of the family, the BTV particle is a non-enveloped, complex virus of two capsids, organized in three layers from outmost VP2 through intermediate VP5 and VP7 to VP3, respectively (Roy, 2001). Cell entry involves virus attachment by VP2 and membrane penetration via VP5 followed by release of the core particle into the cytoplasm (Hassan and Roy, 1999). The released core within the cytoplasm of BTV-infected

* Corresponding author. Department of Infectious and Tropical Diseases, London School of Hygiene and Tropical Medicine, Keppel Street, London WC1E 7HT, UK. Fax: +44-20-7927-2839.

E-mail address: polly.roy@lshtm.ac.uk (P. Roy).

0042-6822/$ - see front matter © 2004 Elsevier Inc. All rights reserved.
doi:10.1016/j.virol.2004.04.018

cells has the ability to transcribe capped mRNA from the viral genomic RNA segments (Roy, 2001). The surface layer of the core is made up of 260 trimers of VP7 (38 kDa) that are organized in icosahedral arrangements. The underneath protein layer is composed solely of the 110-kDa protein VP3 and provides a smooth scaffold for the deposition of VP7 trimers. The X-ray structure of BTV core has revealed that 120 copies of VP3 organized into 12 flower-shaped decamers that are interconnected to form the thin, smooth VP3 shell. While this serves as the scaffold for deposition of VP7 trimers, it also encapsidates and positions the transcriptase complex of three minor proteins (VP1, VP4, and VP6) and closely associates with the genomic 10 dsRNA segments. The functional importance of the VP3 layer is further highlighted by the conservative nature of the overall framework of this shell, which is shared by all members of *Reoviridae* (Grimes et al., 1998; Hewat et al., 1992; Prasad et al., 1992, 1996; Reinisch et al., 2000). In each case, 120 copies of the equivalent protein (λ1 for Orthoreovirus, VP2 for Rotavirus) per core of that virus form the icosahedral shell that packages genome and transcription complex (TC) components. To achieve the icosahedral symmetry in the final assembled layer of BTV VP3, 120 VP3 molecules are arranged into 60 subunits of two distinct types of VP3 (A and B), the final folding of which differs slightly from each other (Grimes et al., 1998). The 901 amino acids of VP3 in each monomer form a large elongated triangular structure, each of which is divided into three distinct domains, named as apical, carapace, and dimerization domains (Grimes et al., 1998). The structure of the VP3 layer shows that around the 5-fold axis a set of five monomers of the VP3 A is arranged like petals of flower while another set of five VP3 B interconnects the five VP3 A petals. The connections between decamers are achieved predominantly via the interactions of the dimerization domains of A and B of different decamers at the local 2-fold axis and through certain subtle changes in conformational rearrangements of A and B molecules. It is therefore highly likely that decamers are the assembly intermediates of the VP3 lattice, although no direct evidence for this has yet been obtained. Unlike the B molecule, the N-terminus of the A molecule cannot be placed accurately, implying it is conformationally flexible, perhaps to accommodate assembly. The N-terminus of Reovirus equivalent protein λ1 has similarly not been placed by X-ray analysis. The crystal structure shows VP3 is associated with genomic dsRNA and indicates the possible locations of the internal proteins that form the transcription complex (TC) of the virion (Grimes et al., 1998). Location of TC at the vertices of the 5-fold axes of the decamers is further supported by demonstrating the release of newly synthesized RNA species through these vertices (Gouet et al., 1999) and direct localization of at least two TC components, the polymerase and the capping enzyme (VP1 and VP4), within the core has been confirmed by high-resolution Cryo-EM analysis (Nason et al., 2004).

To resolve some of the uncertainties of VP3 assembly, we undertook a study in which we investigated the role of N-terminus in VP3 assembly, interaction with TC complex, and VP7 trimers. In addition, we identified the VP3 assembly intermediates and obtained direct evidence of the involvement of dimerization domain in VP3–VP3 interactions in core formation.

Results

Construction and expression of N-terminus deletion mutants of VP3 proteins and their effects on capsid formation

The crystal structure of the BTV core could not resolve the electron density map of the first 56 residues of VP3 A, implying that the N-terminal region of VP3 A has a flexible conformation (Grimes et al., 1998). Such flexibility may be necessary to alter its position from one domain to another during core assembly and transcription processes (Grimes et al., 1998). It is also speculated that this region might be in close contact with the transcription complex, holding at least some of the components in the right orientation near the 5-fold axis (Gouet et al., 1999). To better understand the involvement of the N-terminus in core assembly and its interaction with the minor core proteins VP1 and VP4, we designed two deletion mutants and examined their role in different assay systems. The transfer vectors were constructed and recombinant baculoviruses were generated as described under Materials and methods. Insect cells infected with recombinant baculoviruses were harvested 48 h postinfection (hpi), lysed, and proteins were recovered and analyzed by sodium dodecyl sulphate-10% polyacrylamide gel electrophoresis (SDS-10% PAGE). As controls, both uninfected Hi5 cell lysate and AcNPV-infected cell lysate were also included. Both recombinant viruses expressed the

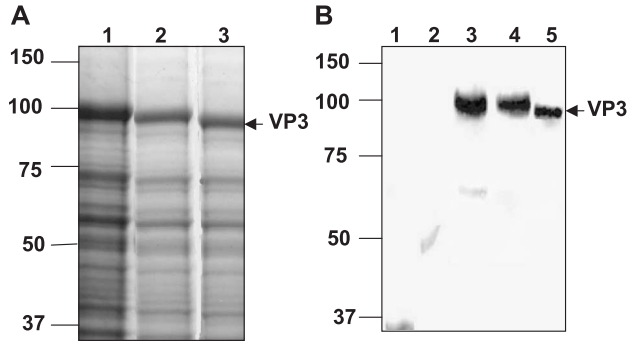

Fig. 1. Expression of VP3 deletion mutants in insect cell. Hi5 cells were infected with each recombinant baculovirus at a MOI of 5 and the cells were harvested 48 h postinfection. Infected cells were lysed; proteins were resolved on a SDS-10% PAGE and stained with Coomassie blue (A) or analyzed by Western blotting (B). (A) Lanes 1, 2, and 3 show the protein profiles of recombinant viruses expressing the WT VP3, Δ5N, and Δ10N, respectively. (B) Lane 1, Baculovirus infected Hi5; lane 2, uninfected Hi5; lane 3, WT VP3; lane 4, Δ5N VP3; and lane 5, Δ10N VP3.

deletion forms of VP3 in insect cells (Fig. 1A). The presence of truncated and wild-type VP3 was confirmed by Western blotting using anti-VP3 antibody (Fig. 1B). The SDS-10% PAGE and Western analysis indicated that the expressed mutant proteins were in soluble form, although the levels of expression were less than the wild-type VP3. It was therefore considered that each of these mutants had similar overall characteristics to those of wild-type VP3.

BTV core-like particles (CLPs) are formed efficiently in the cytoplasm of insect cells when VP3 and VP7 are synthesized by recombinant baculoviruses (French et al., 1990). This approach allows the determination of the effects of mutations introduced into the different viral structural proteins on the particle assembly and structure (Gilbert and Greenberg, 1998; Lawton et al., 1997; Limn et al., 2000; Tan et al., 2001; Tang et al., 2002). We used this assay system to examine the assembly efficiency of each VP3 mutant. A coinfection of VP7 and unmodified VP3 served as a control (Fig. 2A, lane 1). Infected cells were lysed 3 days postinfection and CLPs were purified by CsCl gradient centrifugation as described in Materials and methods. Purified CLPs were analyzed both by SDS-10% PAGE and by electron microscopy. The SDS-10% PAGE clearly demonstrated that Δ5N mutant is capable of forming CLPs in the presence of VP7, although the efficiency was a little less than that of wild-type VP3 protein reflecting VP3 levels (Fig. 2A, lane 2). However, the number of purified CLPs that could be isolated when Δ10N VP3 was used was much less than those CLPs that were generated either using the wild-type or the Δ5N mutant VP3 molecules (Fig. 2A, lane 3). These findings clearly indicate that the efficiency of VP3 and VP7 assembly is affected by deletion of 10 N-terminal residues. The molar ratio of VP3 and VP7 in the Δ5N CLP preparation was estimated by scanning the Coomassie-stained protein bands and demonstrated that this mutant had a ratio of 120 VP3: approximately 600 VP7, identical to the wild-type CLPs as reported previously (Limn and Roy, 2003). It was not possible to isolate enough CLPs with Δ10N VP3 to estimate the number of VP3 and VP7 unequivocally. The morphology of purified Δ5N CLPs was examined by EM analyses of negatively stained particles. The arrangement of VP7 capsomers in the outer layer of these purified particles appeared more or less dense and regular, similar to wild-type CLPs (Fig. 2B).

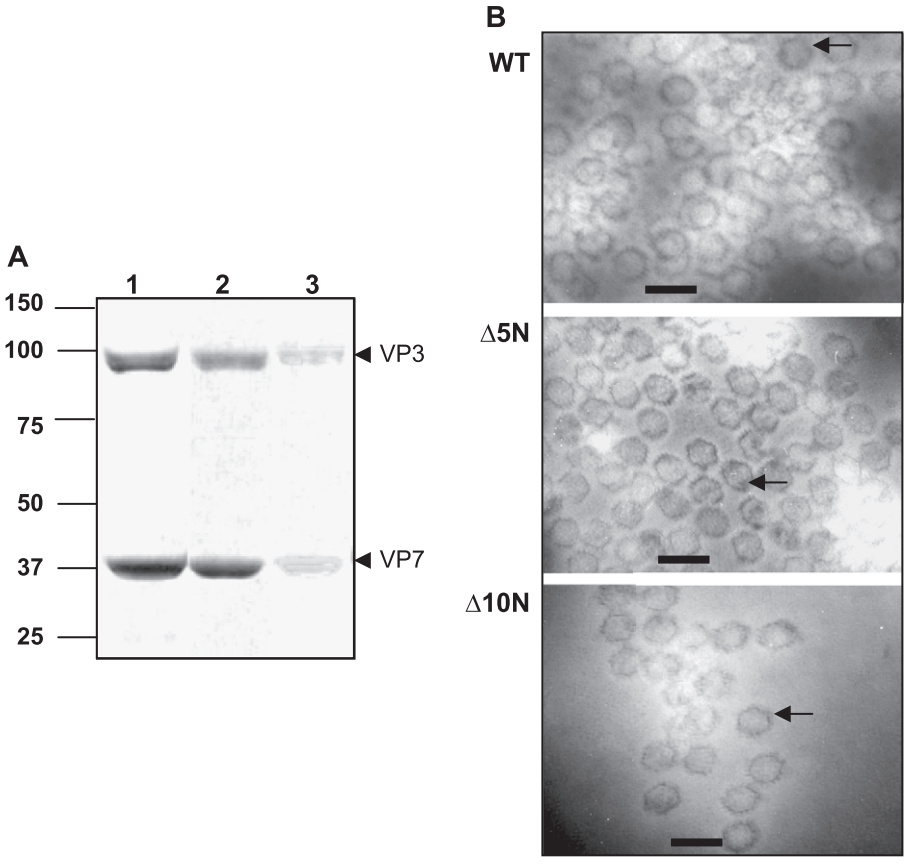

Fig. 2. Protein analysis of purified CLP. Hi5 cells were coinfected with AcBTV-10 VP7 and either AcBTV17-3 or recombinant baculoviruses expressing Δ5N VP3 or Δ10N VP3 proteins. Infected cells were harvested 48 h postinfection, lysed, and the expressed particles were purified on a CsCl gradient centrifugation. Particulate fractions were analyzed either by SDS-10% PAGE followed by Coomassie blue staining (A) or by EM (B). Panel A shows the CLPs formed by VP7 with native VP3 (lane1) or with Δ5N (lane 2) and Δ10N (lane 3). The positions of VP3 and VP7 are indicated. (B) Electron micrographs of CLPs by negative staining. CLPs formed by wtVP3, Δ5N, and Δ10N mutants are indicated. Arrangement of VP7 capsomers was indicated by the arrow in each panel. Scale bar is equivalent to 100 nm.

Do CLPs assembled by deletion mutants of VP3 retain the ability to encapsidate the internal minor proteins?

It has previously been established that in insect cells, BTV CLP formed by VP3 and VP7 proteins incorporates minor core proteins VP1 and VP4 in a ratio identical to the authentic core, when co-expressed with appropriate recombinant baculoviruses (Le Blois et al., 1992; Loudon and Roy, 1991). Our recent biochemical data together with the Cryo-EM studies of CLPs formed by VP1, VP3, VP4, and VP7 indicated that VP3 may have direct interactions with the VP1 and VP4 complex (Nason et al., in press). To determine if the N-terminal deletion of VP3 has any effects on VP1 and VP4 encapsidation within the CLPs, *Spodoptera frugiperda* (*Sf9*) cells were co-infected with recombinant viruses expressing VP7, truncated VP3 (Δ5N) proteins together with recombinant viruses expressing VP1 or VP4. After 3 days of infection, CLPs were isolated from infected cells and analyzed by SDS-10% PAGE. For controls, a recombinant virus expressing wild-type VP3 was used for co-expression studies. VP1 and VP4 were encapsidated as expected within the CLPs formed by wild-type VP3 in a ratio equivalent to the authentic core (Fig. 3A, lane 1). Both minor proteins were also incorporated into the CLPs when they were generated with Δ5N VP3 and wild-type VP7, and that the levels of VP1 and VP4 were equivalent to that of wild-type (Fig. 3A, lane 2). The authenticity of BTV proteins was confirmed by Western analysis using anti-BTV antisera as shown (Fig. 3B). The data indicate that the first five residues of VP3 protein are not necessary for the incorporation of these two minor core proteins underneath the VP3 layer.

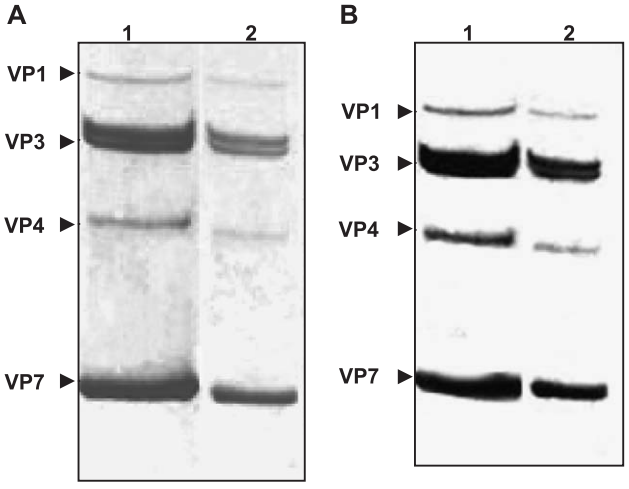

Fig. 3. Encapsidation of minor core proteins by CLPs. Hi5 cells were coinfected with AcBTV-10 VP7 and either with AcBTV17-3 or recombinant baculovirus expressing Δ5N VP3 protein together with AcBTV10-VP1 (expressing VP1) and AcBTV10-VP4 (expressing VP4) as described in Materials and methods. Infected cells were harvested at 48 h postinfection, lysed, and the expressed particles were then purified on a CsCl gradient centrifugation and analyzed either by SDS-10% PAGE followed by Coomassie blue staining (A) or by Western blot analysis (B) using anti-BTV polyclonal antibody. Lane 1, CLPs formed by wtVP3; and lane 2, CLPs formed by Δ5N. Positions of each BTV proteins are indicated.

Expression and purification of an assembly deficient internal deletion mutant (ΔDD VP3) that lacks the VP3 dimerization domain

Structural data indicate that aa 699–854, towards the carboxyl end of VP3, are responsible for the joining A and B molecular forms of VP3 at the 2-fold axis between the decamers and thus denoted as ''dimerization domain'' (Grimes et al., 1998). To investigate whether the VP3 decamers are indeed the assembly intermediates for the VP3 shell assembly, we designed a deletion mutant lacking the interconnecting 155 residues (aa 699–854) of VP3. This deletion mutation in VP3 should disrupt the dimer formation between the A and B molecules at the 2-fold axis, thereby inhibiting the decamer–decamer interaction but should not perturb the assembly of decamers themselves, if they are a true intermediate. A recombinant baculovirus was prepared expressing the ''dimerization domain''-deleted VP3 protein (ΔDD VP3) as described in Materials and methods. When insect cells infected with the recombinant virus expressing the ΔDD VP3 were analyzed by SDS-10% PAGE, both Coomassie-stained gel (Fig. 4A) and Western blotting (Fig. 4B) showed a distinct VP3 band that was smaller than the parental VP3 band and had an estimated size of 81 kDa. To examine the core assembly proficiency of this mutant, insect cells were co-infected with this recombinant virus (ΔDD VP3) along with the recombinant virus expressing VP7 and the particle formation was assessed. As expected, no particles could be detected either by EM analysis of the infected cells or by gradient purification of the soluble fraction obtained from the infected cell lysates. The mutant completely abolished the formation of the VP3 shell and consequently CLP assembly (data not shown).

To characterize the mutant protein in detail, the ΔDD VP3 protein was overexpressed in Hi5 insect cells and harvested at 48 h postinfection. Sequential chromatography as described in Materials and methods isolated VP3 to more than 85% pure as estimated by SDS-10% PAGE (Fig. 4C). The identity of VP3 was confirmed by Western blot analysis using anti-VP3 antibody (Fig. 4D).

Deletion of dimerization domain forms distinct multimers in solution

The oligomeric status of semi-purified ΔDD VP3 was determined by gel filtration on a Superdex 200 column calibrated using a set of globular protein standards (Amersham Pharmacia Biotech) consisting of thyroglobulin (669 kDa), ferritin (440 kDa), catalase (232 kDa), lactate dehydrogenase (140 kDa), and BSA (67 kDa). The collected fractions exhibited two major peaks, one was eluted in the void volume ahead of the 669-kDa marker protein and the other was present in the 160-kDa region in addition to other

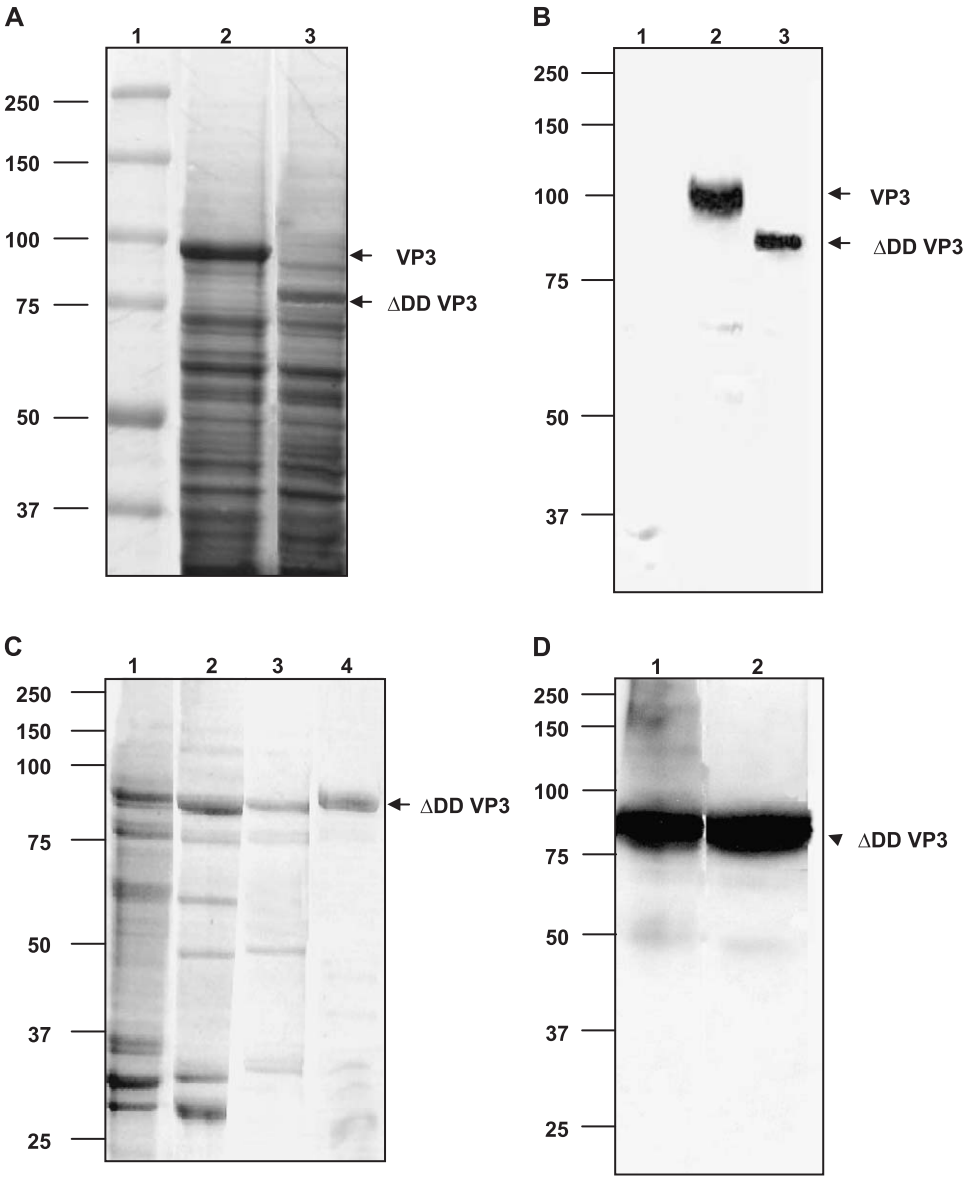

Fig. 4. Expression and purification of recombinant ΔDD VP3. Hi5 cells were infected with each recombinant baculovirus at a MOI of 5, and the cells were harvested at 48 h postinfection, lysed, and proteins were resolved on a SDS-10% PAGE, followed by staining with Coomassie blue (A) or by Western blotting using polyclonal anti-BTV VP3 antiserum (B). Lane 1, marker proteins; lanes 2 and 3, recombinant viruses expressing the wt VP3, and ΔDD VP3, respectively. (C) ΔDD VP3 was purified from infected cell lysates using column chromatography as described in Materials and methods. Aliquots from each purification step were analyzed on a SDS-10% PAGE followed by Coomassie blue staining. Lane 1, ΔDD VP3 cell supernatant after homogenization; lane 2, supernatant after ammonium sulphate precipitation; lane 3, fractions after Hi trap SP column; lane 4, fractions after Superdex 200 gel filtration column. (D) Western blot analysis of ΔDD VP3 using polyclonal anti-BTV VP3 antiserum. Lane 1, ΔDD VP3 after ammonium sulphate precipitation; lane 2, purified ΔDD VP3.

minor peaks (Fig. 5A). The first peak corresponds to a high-order multimer and represented a molecular size of VP3 decamer and the slower migrating peak corresponded to the size of VP3 dimer lacking the 155 residues in each molecule. On a SDS-10% PAGE, both these two peaks as well as fractions from other peaks migrated at the position of approximately 81 kDa (see Fig. 5A, lower panel). To obtain confirmation that the presence of VP3 oligomers in these fractions and to identity the types of oligomer (i.e., dimer and decamer), the eluted fractions were analyzed on a 2.5% native polyacrylamide gel, which separates the protein from its charge as well as the hydrodynamic size. The migration patterns of the VP3 fractions clearly indicated that the higher multimer had a size of a VP3 decamer (Fig. 5B, lane 2) while the faster band had a size of a VP3 dimer (Fig. 5B, lane 1).

VP3 without the dimerization domain assembles as decamer structures and is visualized as particulate structures

The results obtained above clearly demonstrate that complete removal of the dimerization domain allows for-

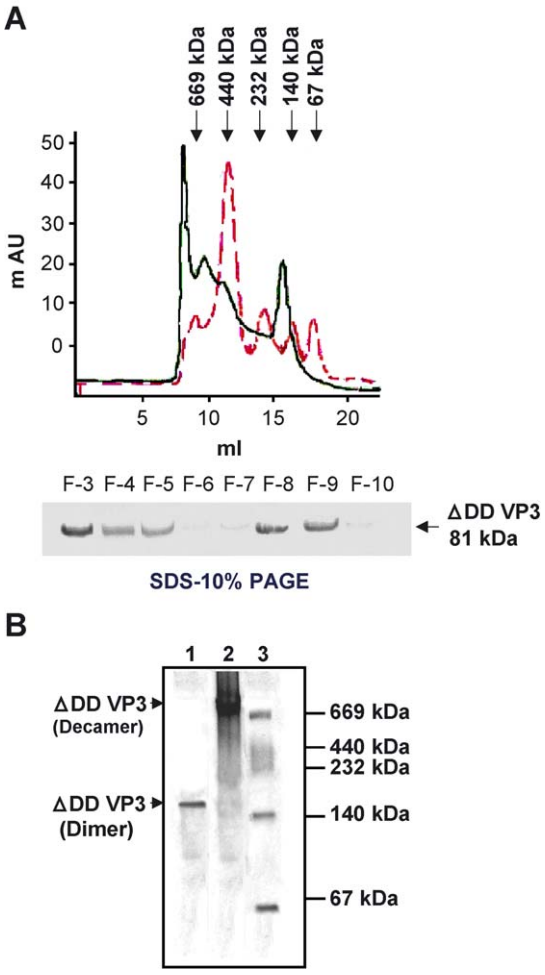

Fig. 5. Gel filtration chromatography and native gel electrophoresis of ΔDD VP3 oligomer. (A) Chromatogram showing the elution profile of ΔDD VP3 oligomers (upper panel). Purified protein was loaded onto a pre-equilibrated column as described in Materials and methods, and protein was eluted at a flow rate of 0.3 ml/min. The column was calibrated using a set of globular protein standards consisting of thyroglobulin (669 kDa), ferritin (440 kDa), catalase (232 kDa), lactate dehydrogenase (140 kDa), and BSA (67 kDa). Sizes of eluted markers are indicated. Protein fractions were collected (upper panel) and separated on a SDS-10% PAGE (lower panel). Two major peaks of ΔDD VP3 were eluted, one between the 232- and 140-kDa markers positions and the other in the void volume, larger than the 669-kDa marker (upper panel). (B) Native gel electrophoresis (10%) of ΔDD VP3 fractions stained with Coomassie blue. Fractions containing the slower migrating peak show the size equivalent to dimer of ΔDD VP3 (lane 1, indicated as 'dimer') and the faster peak eluted in the void volume has the size of ΔDD VP3 decamer (lane 2, indicated as 'decamer'). Pharmacia high molecular weight markers were used as standard (lane 3).

mation of VP3 multimers in solution. To elucidate the precise nature of the multimeric forms, we employed different biophysical techniques including analytical ultracentrifugation, electron cryo-microscopy (Cryo-EM), and dynamic light scattering.

The decamer fractions obtained from the above gel chromatography were subjected to sedimentation velocity analysis using the Beckman XL-A analytical centrifuge. For boundary sedimentation analysis, the protein was used at a concentration range of 0.3 mg/ml and centrifuged at 40 K rpm as described in Materials and methods. Analytical data indicated that the higher multimers had the sedimentation coefficient of approximately 13S, comparable to the decameric form of the mutant protein, which has an apparent molecular weight of 820 kDa (Fig. 6A). However, in addition to decamer species, two other major protein species with sedimentation coefficients equivalent to VP3 monomers and dimers were also present. The data indicated that oligomers were in a dynamic state of equilibrium and that the isolated decamers dissociated readily when centrifuged at high speeds (40 K). Dynamic light scattering (Dynapro) of the recombinant protein was also in agreement with the critical mass shown by the analytical centrifugation study (data not shown).

To investigate the morphology of purified decamers, we examined the purified protein by conventional negative staining followed by EM analyses as described in Materials and methods. Negative staining of the protein exhibited aggregates in the micrograph without any definite structure (data not shown), probably due to the sensitivity of the oligomers to the EM fixatives used. To avoid these artifacts, the cryo-microscopy technique was employed. Micrographs obtained from the Cryo-EM study exhibited the presence of smooth circular ring-like structures (Fig. 6B) whose dimensions were consistent with the VP3 decamers as seen by structural studies of the BTV core (Grimes et al., 1998).

ΔDD VP3 could still interact with VP1 and VP4 but lost RNA binding activity

The dimerization domain deleted VP3, retains the intact amino terminus, and thus should include the interacting ability with the minor proteins that are located underside of the VP3 layer at the 5-fold axis of the shell. To examine this, *Sf9* cells were infected with three recombinant baculoviruses expressing VP1, VP4, and truncated VP3 or wild-type VP3 in presence of [^{35}S]-Met/Cys. To identify the protein complexes formed between VP3 and VP1–VP4, radiolabeled recombinant BTV proteins present in the soluble fraction were separated from the infected cell debris, and the protein complexes formed between VP3 and VP1 or VP4 were immunoprecipitated with anti-BTV VP3 antiserum. The interacting proteins were then analyzed by SDS-10% PAGE followed by autoradiography. From this analysis, it was evident that the decamers could interact with both minor proteins equally well (Fig. 7A). These biochemical data support the prediction of X-ray structural studies as well as our recent data obtained from Cryo-EM studies that show the location of the TC at the 5-fold vertices of the subcore, and not at the decamer–decamer interacting site (Grimes et al., 1998; Nason et al., in press).

Our data confirmed that VP3 decamers were closely associated with two of the TC components; however, to assess if decamers also interacted with the genomic RNAs, we labeled the 10 segments of BTV dsRNA with 5′-^{32}P

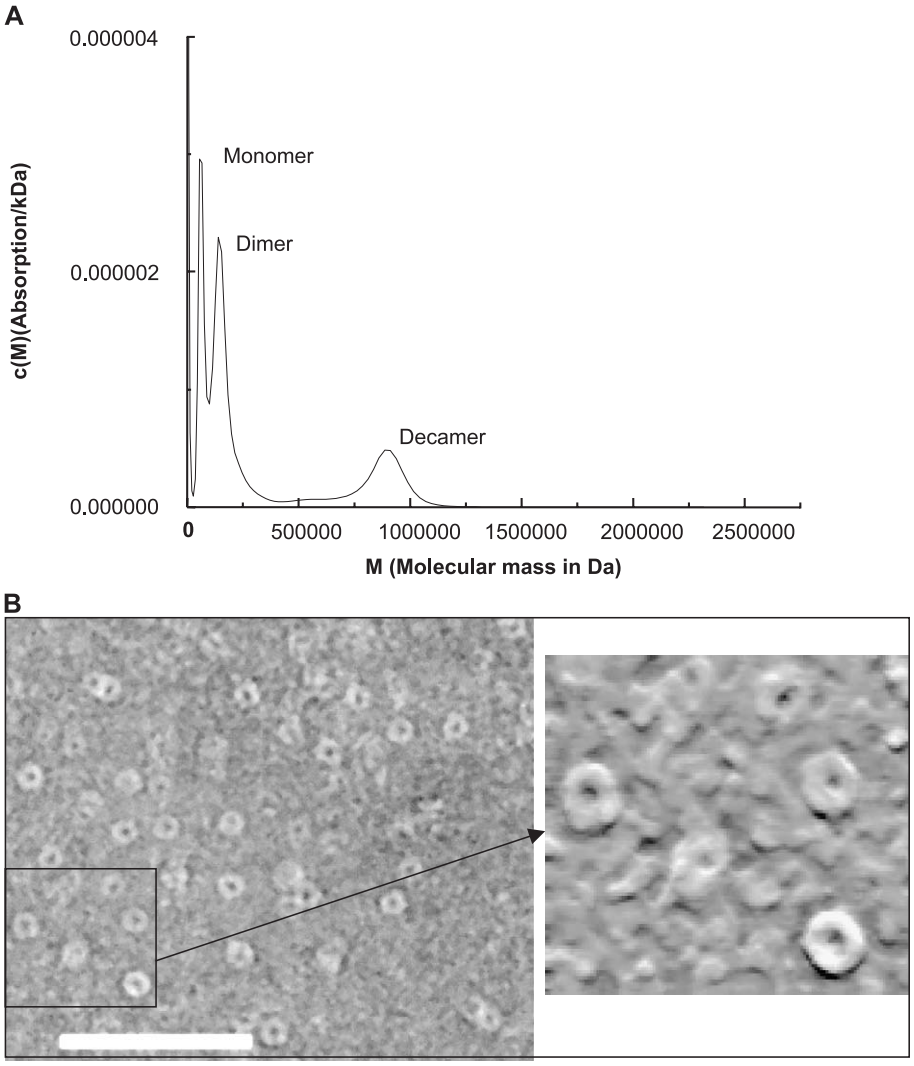

Fig. 6. Sedimentation velocity analysis and cryo-electron microscopy of the purified ΔDD VP3 protein. (A) Sedimentation velocity experiments were performed using a Beckman Model XL-A centrifuge using a 0.3-cm path length double sector cells with quartz windows. Recombinant protein was diluted to 0.3 mg/ml with 20 mM Tris–HCl (pH7.5), 50 mM NaCl, and centrifuged at 40 000 rpm. (B) Purified protein for cryo-microscopy was embedded in a thin layer of vitreous ice on glow-discharged holy carbon films using standard procedure (Dubochet et al., 1988; Hewat et al., 1992). Frozen hydrated specimens were imaged in a Jeol 1200 electron cryo-microscope using a 100-kV electron beam at a magnification of 60 000×. Arrow heads indicate the particle. Small panel shows the enlarged particle. Scale bar indicates 100 nm.

cytidine triphosphate and assayed binding with purified decamers. When the RNA–VP3 complexes were monitored by gel shift assay on 4% PAGE, unlike the whole VP3 protein which could shift the dsRNA very efficiently, the VP3 decamers exhibited no RNA binding activity (Fig. 7B) in agreement with the structural data, which indicated that the dimerization domain of VP3 and interactions between the VP3 decamers are probably directly associated with genomic RNA located inside the core.

Discussion

Viral capsid assembly is a precise process that is fundamental to the success of the viral infection. In recent years, the assembly of the inner capsid or core of various members of the *Reoviridae* family has been a major focus at both the structural and molecular levels. The assembly of multilayered viral cores is especially intriguing as both protein–protein and protein–RNA interactions are required to complete the core particle. Recently, we conducted studies on the complex assembly pathway of the 260 VP7 trimers that form the surface layer of the BTV core. In this report, we analyze the assembly process of the VP3 layer itself with a view to describing the nature of the intermediates and the functional basis of the encapsidation of the minor structural proteins and the 10 segments of the viral dsRNA genome.

The highly conservative nature of the VP3 sequence across 24 BTV serotypes as well as considerable similarities with the sequence of other related Orbiviruses (EHDV and AHSV) (Iwata et al., 1992, 1995; Roy, 1996) highlights the structural importance of this protein. VP3 is considerably

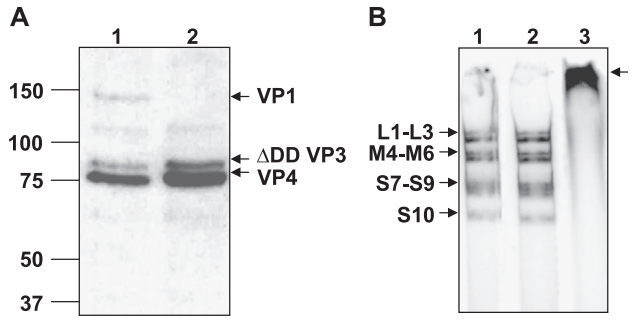

Fig. 7. Interaction of ΔDD VP3 with minor core protein VP1, VP4, and BTV dsRNA segments. (A) Autoradiogram shows the interactions between ΔDD VP3 and VP1, VP4. Hi5 cells were infected with recombinant baculoviruses expressing ΔDD VP3, VP1, and VP4 (lane 1), or only ΔDD VP3 and VP4 (lane 2). Infected cells were radiolabeled at 30 hpi for 2 h with ^{35}S-methionine as described in Materials and methods. Complexes were immunoprecipitated from harvested cell lysates using anti-BTV VP3 polyclonal antibody, analyzed by SDS-10% PAGE, and subjected to autoradiography. (B) Gel shift assay of VP3–RNA interaction; 5 μg of purified ΔDD VP3 (lane 2) or semi-purified wt VP3 (lane 3) was incubated with ^{32}P-labeled 10 BTV RNA segments at room temperature and the mixture was analyzed by EMSA as described in Materials and methods. Labeled RNA alone (lane 1) was used as a control. Note that there is no retardation of BTV RNA segments (L1–L3, M4–M6, S7–S10) in lanes 1 and 2. Arrow indicates retarded migration of RNA.

larger (100 kDa) than the VP7 molecule (38 kDa) and, even before its structural description, was clearly a multifunctional protein. The arrangements of the VP3 molecules within the core, as seen in the final structure (Grimes et al., 1998), consist of 120 molecules organized as 60 dimers. Dimerization is such that each dimer consists of two types of VP3 monomers (A and B) distinguishable by the visible electron density of the extreme amino terminus. In molecule A, the amino terminus is disordered, while in molecule B the electron density is clear (Grimes et al., 1998). The disorder in VP3A is proposed to accommodate the minor rotation of the apical domain but the main body of the protein that allows assembly via a proposed decameric intermediate. To vindicate this model, we sought biochemical support for the crucial role of the amino terminus in assembly.

N-terminal residues have also been studied in several homologous proteins from the *Reoviridae* family (Kim et al., 2002; Zeng et al., 1998). Like the N-terminal 56 residues of BTV VP3 protein, the 230 N-terminal residues of orthoreovirus λ1 are not clearly resolved by X-ray crystallography (Reinisch et al., 2000), and similarly, the N-terminal 89 residues of rotavirus VP2 are also not clearly located by the Cryo-EM (Lawton et al., 1997). The 230 N-terminal residues of λ1 and 89 residues of rotavirus VP2 are dispensable (Dryden et al., 1998; Zeng et al., 1998) for viral core formation; but the intact VP2 N-terminus is needed for the incorporation of VP1 and VP3 and as well as for RNA binding (Labbe et al., 1994; Shaw et al., 1996). In contrast to the $T = 2$ layer proteins of rotavirus and reovirus, our study revealed that the N-terminal sequences of BTV VP3 are critical for the assembly process. Although the loss of five residues from the amino terminus of VP3 still allowed VP3–VP7 core assembly, the loss of 10 residues significantly affected the efficiency of the assembly process as CLP production by the Δ10N mutant was visibly less than either the wild-type VP3 or the Δ5N mutant, and those particles that were formed were very fragile. VP3 has a particularly high hydrophobic amino acid content (Purdy et al., 1984), but several internal of hydrophobic stretches could be deleted without much effect on CLP formation (Tanaka and Roy, 1994). Moreover, these regions could also accommodate insertion of short foreign sequences. Similarly, deletion of 10 residues at the carboxy terminus did not affect the VP3–VP3 and VP3–VP7 interaction and the formation of CLPs (Tanaka et al., 1995). In addition to the assembly of the core, incorporation of the internal minor core proteins was also unaffected for the Δ5N mutation; VP1 and VP4 being encapsidated within the CLPs by Δ5N mutant protein a ratio equivalent to that of cores assembled using parental VP3. Thus, despite a suggested role in binding the transcription complex at the 5-fold axis of the core, our studies suggest that at least the N-terminal five residues of the VP3 N-terminus are not important for this function. The fragility of the CLPs formed using the Δ10N mutant prevented a specific examination of the role of amino acids 5–10 in the same process.

Deletion of 89 residue of rotavirus VP2 self-assembled to make a complete particle, but a complete N-terminus was needed for the incorporation of the minor core proteins (Zeng et al., 1998). Likewise in orthoreovirus λ1, although 230 residues are dispensable for particle assembly, they are proposed to be involved in the binding and encapsidation of RNA (Kim et al., 2002; Labbe et al., 1994), like rotavirus VP2.

The dimerization domain composes a pair of β-sheets, perpendicularly arranged between the A and B molecules, forming a β-sandwich. Decamers are clipped together by weak interactions of the dimerization domain that is truly quasi-equivalent in nature. Five monomers of the VP3A are arranged like petals of a flower and another set of five VP3B are interconnected in between the first set. Twelve such decamers connected together via the interaction of the dimerization domain between the decamers to form a stable particulate subcore structure. A key question, however, is whether the decamer present in the final assembled particle is an identifiable intermediate in the assembly process or only arises upon assembly. To gauge this, we deleted the dimerization domain and showed abolition of subcore formation, consistent with the interaction between the decamers via this region. The deletion of this domain, however, did not perturb decamer or dimer formation as shown by analytical centrifugation and native gel electrophoresis. The ΔDD VP3 mutants could be easily isolated by gentle purification (e.g., gel filtration chromatography). Decamers were highly stable but easily dissociated to monomers and dimers during high-speed (40 000 rpm) centrifugation. The

decamers also dissociated and formed aggregates when treated for conventional microscopic studies. Hence, it seems likely that the decamers are in a dynamic equilibrium state with other multimers and can be shown as monomers, dimers, pentamers, decamers, and higher oligomers, presumably due to their hydrophobic nature. The presence of a higher order of decamers was particularly evident from the Cryo-EM and dynamic light scattering experiments as proteins were maintained in their most native state in the solution.

By using direct protein–protein pull-down assays, we demonstrated that the ΔDD VP3 mutant retained the ability to interact with the minor proteins VP1 and VP4, suggesting that the decamers, as assembly intermediates, are most likely involved in the recruitment of the minor core proteins before complete assembly of the VP3 subcore. We also showed that unlike minor proteins, BTV RNAs did not bind the decamers under conditions where the intact VP3 bound RNA very efficiently. This is entirely consistent with the model of Gouet et al. (1999), which suggested the position in VP3 compatible with RNA–protein interaction lays in a single loop in VP3, the βJ/βK loop (residues 790–817) within the dimerization domain (Grimes et al., 1998).

Our data suggest that decamers are the first stable assembly intermediates of the virion and that VP3 incorporates VP1 and VP4 at this stage (see Fig. 8). The viral genome, by contrast, wraps around the VP1–VP4 complex while the subcores are assembling. Our data suggest that infectious BTV entirely assembled in vitro, may be a realistic possibility as further aspects of the assembly pathway become equally clear.

Materials and methods

Virus and cells

Autographa Californica nuclear polyhedrosis virus (ACMNPV) and the recombinant baculoviruses were propagated in the *Spodoptera frugiperda* (*Sf9*) insect cell line or Hi5 insect cell line (Invitrogen) at 28 °C in serum-free SF900 ll medium (GIBCO) as described elsewhere (King L.A., 1992).

DNA manipulation and construction of DNA clones

Plasmid DNA manipulation was done essentially as described by Sambrook and Russell (2001). Restriction enzymes, T4 DNA ligase, and DNA polymerase were purchased from New England Biolab (NEB). Calf intestinal alkaline phosphatase was obtained from Boeringer GMBH (Mannheim, Germany).

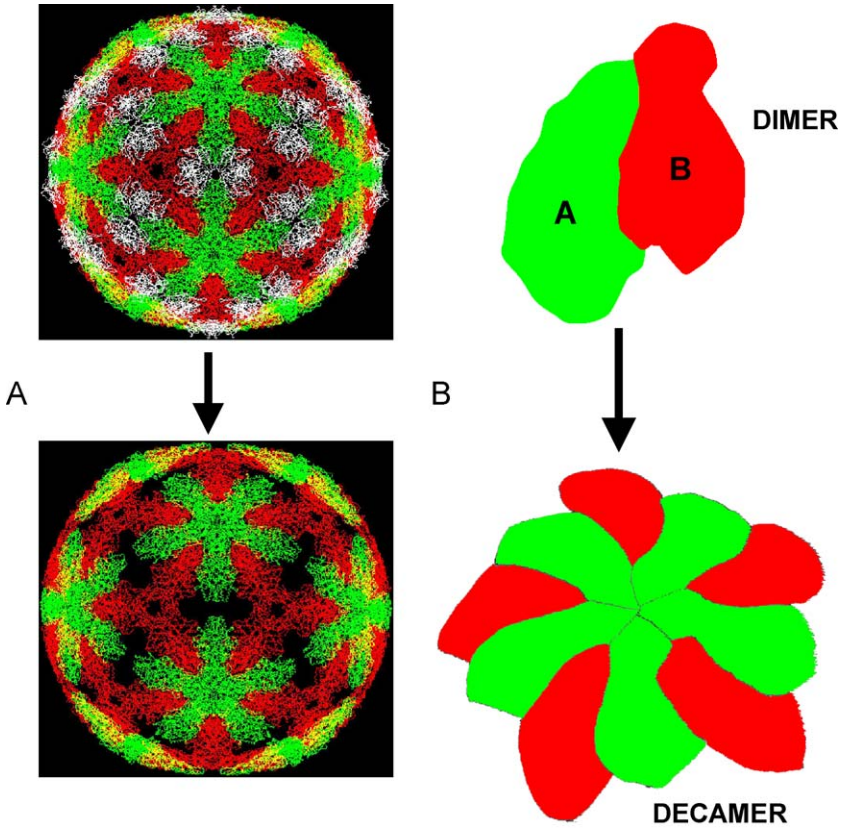

Fig. 8. Schematics of VP3 shell and VP3 oligomers. The cartoons are adapted from the published report of Grimes et al. (1998). (A) VP3 shell shows the dimerization regions in each molecule in white (upper panel) and deletion of dimerization regions (lower panel). Panel (B) shows a dimer and a decamer of VP3.

Construction of mutant VP3 genes and generation of recombinant baculoviruses expressing mutant VP3 proteins

Generation of a modified pAcYM1 vector containing SmaI restriction enzyme site

The baculovirus-compatible pAcYM1 vector has the *Bam*HI insertion site downstream of the polyhedrin promoter region for the incorporation of foreign genes. Because the BTV-17 VP3 gene has two internal *Bam*HI sites (Ghiasi et al., 1985), an alternate restriction site, *Sma*I downstream of the *Bam*HI site, was incorporated. Synthetic *Bam*HI–*Sma*I adaptor oligonucleotide 5′-d (GATCCCCGGG) was used for this purpose and was obtained from Amitof Biotech Inc. (MA). The oligonucleotide was then phosphorylated, annealed, and ligated to *Bam*HI-digested pAcYM1 vector to add *Sma*I site adjacent and 3′ to the *Bam*HI site.

Construction of N-terminal deletion mutants

For the generation of the N-terminal 5 and 10 amino acid deletion mutants of VP3, we have used cDNA of the BTV-17.3 gene that was inserted previously in the *Sma*I site of the plasmid vector pGEM3Zf(+). Appropriate forward primers containing the *Sma*I site and the start codon ATG (5-CGC*CCCGGG*CAGATGGAGCAACGTCCG-3′ for the BTV-17.3Δ5N mutant, and 5′-CGC*CCCGGG*CCGATGCCGAATAAAGACGACG-3′ for the BTV-17.3Δ10N mutant) were designed. The reverse primer in both cases was the SP6 sequence (5′-GCGATTTAGGTGACACTATA-3′) in the polymerase chain reaction (PCR). Subsequent sequencing of this portion of the BTV-17.3Δ5N and Δ10N mutants was then confirmed by the dideoxynucleotide technique (Sanger et al., 1977) using a T7 sequenase version 2.0 dGTP reagent kit (Amarsham, Life Science, Cleveland, OH, USA).

Construction of VP3 dimerization domain deletion (BTV-17.3 ΔDD) mutant

To generate BTV-17.3ΔDD mutant, we employed a total of three polymerase chain reactions (PCRs) to generate a short fragment lacking the dimerization domain (nt 2111 to 2579) but having minimal flanking sequences of the domain. We chose two unique restriction enzyme sites *Psh*AI and *Bgl*I, residing at nucleotides 1865 and 2703, respectively, with an expected amplified product of 370 base pair length. The full-length cDNA of BTV-17.3 in baculovirus-compatible pAcYM1 plasmid was used as template for the first and second rounds of PCR reactions. The first round of PCR was done by using a forward primer (5′-TTC GAA GAT CTG ATG AAG AGA ATT GTT GAG-3′) and reverse primer (5′-GCA *GCC AGCTTG GC*G CCC-3′) with *Bgl*I site. The second round of PCR used the forward primer 5′-TGC *GAC ACT TGT C*AT TAA-3′ with a *Psh*AI sequence and a reverse primer 5′-CTC AAC AAT TCT CTT CAT CAG ATC TTC GAA-3′ (representing anti-codons for the aa 859–855, 698–694 of the VP3 protein). The final round of PCR utilized the mixture of PCRI and PCRII as template and the selected primers used in the earlier reactions. The reverse primer of PCRI encoding the *Bgl*I sequence was used along with the forward primer of PCRII encoding the *Psh*AI sequence. The resulting PCR-amplified fragment now contained both *Psh*AI and *Bgl*I restriction sites. This product was double digested with *Psh*AI and *Bgl*I, gel purified, ligated with *Psh*AI and *Bgl*I, digested, dephosphorylated pAcYM1.17.3 plasmid, and sequenced to generate the BTV-17.3ΔDD mutant.

Generation of recombinant baculoviruses

The lipofection technique was used to co-transfect monolayers of *Sf9* cells with the recombinant transfer vectors, all generated as described above and *Bsu*36I triple-cut AcNPV DNA (Kitts and Possee, 1993). Recombinant baculoviruses were selected from their *LacZ*-negative phenotypes, plaque purified, and propagated as described elsewhere (Felgner et al., 1987).

Protein analysis

Confluent monolayers of Hi5 cells in 35-mm tissue culture dish were infected with recombinant virus at a multiplicity of infection (MOI) of 5. At 48 h postinfection, cells were harvested and lysed in 150 μl of lysis buffer (50 mM Tris–HCl [pH 8], 200 mM NaCl, 1% Triton X-100). Protein samples (20 μl) were boiled for 6 min in 5× sample buffer (2.3% SDS, 2.5% [vol/vol] glycerol, 5% [vol/vol] β-mercaptoethanol, 62.5 mM Tris–HCl [pH 6.8], 0.01% bromophenol blue), and proteins were separated on a sodium dodecyl sulphate 10% polyacrylamide gel electrophoresis (SDS-10% PAGE) and stained with Coomassie blue.

Immunoblot analysis

For Western blot analysis, proteins were transferred from gels onto a poly-vinyl difluoride (PVDF, Millipore international) membrane by semidry blotting procedure. Membranes were incubated with the anti-BTV10 antiserum diluted 1:1000 in blocking buffer (containing 5% [wt/vol] skim milk and 0.1% [vol/vol] Tween 20 in PBS), followed by incubation with secondary antibody conjugated with horseradish peroxidase (HRP), and developed with ECL chemiluminescence kit (Amarsham-Pharmacia) as directed by vendor.

Labeling of baculovirus-infected insect cells and immunoprecipitation

Sf9 cells were infected with one or two recombinant baculoviruses at a MOI of 5 and incubated in serum-free SF900 II media at 28 °C. After 30 h post infection (hpi), cells were pulsed with 100 μCi of ^{35}S-Met/Cys (NEN) for 2 h. Cells were then harvested, washed, and lysed with

radio-immunoprecipitation (RIPA) buffer (50 mM Tris–HCl [pH 7.5], 150 mM NaCl, 1% Triton X-100, 0.5% sodium deoxycholate, 1 mM EDTA), incubated in ice for 15 min, and centrifuged at 13 000 × *g*. Cell lysates were incubated with an anti-VP3 polyclonal antiserum and the complex was precipitated with protein A agarose beads (Pierce), washed with RIPA buffer, analyzed by SDS-10% PAGE, and auto-radiographed.

BTV dsRNA labeling with ^{32}P-cytidine triphosphate

BTV 10 dsRNA was purified by standard method and labeled with ^{32}P cytidine bis-diphosphate (pCp) and RNA ligase according to the method described elsewhere (Mertens et al., 1987). Briefly, 10 μg of BTV10 RNA was incubated with 10 μCi ^{32}P-cytidine bis-diphosphate (NEN Life Science) in the presence of 10 U of RNA ligase and incubated overnight at 4 °C. Labeled dsRNA was separated from the unincorporated label by using Microspin S-200 high resolution columns (Amersham Pharmacia) as recommended by the manufacturer.

Purification of core-like particle

Baculovirus-expressed CLPs were purified as described previously (French et al., 1990). Briefly, *Sf9* cells were coinfected with recombinant baculovirus in suspension culture with wild-type VP7 (Oldfield et al., 1990) together with either wild-type VP3 (Marshall and Roy, 1990) or mutant VP3 using 5 MOI per cell. After incubation at 28 °C for 48 h, infected cells were harvested and lysed by Dounce homogenization in TNN buffer (200 mM Tris–HCl [pH 8], 150 mM NaCl, and 0.5% [vol/vol] nonidet P-40). Assembled CLPs were purified from the soluble fraction by centrifugation on a 35% CsCl gradient. The presence of protein was analyzed by SDS-10% PAGE followed by Coomassie brilliant blue staining.

Purification of dimerization domain deleted VP3 (ΔDD VP3)

Hi5 insect cells were infected with recombinant ΔDD VP3 at 5 MOI/cell and incubated in serum-free SF900 II medium for 48 h at 28 °C. All subsequent operations were performed at 4 °C unless otherwise stated. Cells were harvested and disrupted by Dounce homogenization in lysis buffer (50 mM Tris–HCl [pH 8], 200 mM NaCl, 1 mM EDTA, 1% [vol/vol] nonidet P-40, 5 mM dithiothreitol (DTT), 1 mM PMSF, and complete protease inhibitor mixture (Boehringer)). The insoluble material was pelleted at 27 000 × *g* for 30 min in a Sorvall SS34 rotor. Clarified supernatant was precipitated with 40% saturated ammonium sulphate and then centrifuged at 40 000 × *g* for 30 min. The resulting supernatant was then adjusted to 65% saturated ammonium sulphate and centrifuged at the same speed as above. The precipitate was resuspended in a minimal volume of 20 mM Tris–HCl [pH 6.8], 20 mM NaCl. After clarification, the sample was loaded onto a 5 ml HiTrap SP (Pharmacia) column previously equilibrated with 20 mM Tris–HCl [pH 6.8], 20 mM NaCl. Bound proteins were eluted by using a sodium chloride gradient (20 mM to 1 M in 20 mM Tris–HCl [pH 6.8]). Fractions containing the protein were pooled and buffer changed to 20 mM Tris–HCl [pH 7.5], 20 mM NaCl by ultra filtration with centrico-30 device (Amicon), and loaded onto a Superdex 200 (Pharmacia) gel filtration column previously equilibrated with the same buffer. Proteins were eluted at a flow rate of 0.3 ml/min by isocratic elution with the same buffer. Fractions containing the VP3 protein were pooled, concentrated, and stored at −70 °C until further use.

Native gel electrophoresis

Purified ΔDD VP3 was resolved in 9% native acrylamide gel (375 mM Tris–HCL, pH 6.8), 3% native stacking gel (125 mM Tris–HCl, pH 6.8), and using electrophoresis buffer without SDS (25 mM Tris and 200 mM glycine). Protein samples were mixed with 50% glycerol, 0.2% bromophenol blue, and loaded for separation. High molecular weight calibration kit (Pharmacia) for native gel electrophoresis was used. The marker consists of thyroglobulin (669 kDa), ferritin (440 kDa), catalase (232 kDa), lactate dehydrogenase (140 kDa), and BSA (67 kDa). Electrophoresis was carried out at constant voltage until the dye migrated to the bottom of the gel.

Gel filtration chromatography

The molecular weight of ΔDD VP3 was determined on a Hi-Load 16/60 Superdex 200 column (Pharmacia). The column was equilibrated with 20 mM Tris–HCl (pH 7.5) and 20 mM NaCl before loading of the protein samples. The protein was eluted with the same buffer at a flow rate of 0.3 ml/min. Protein-containing fractions were analyzed by SDS-10% PAGE. Column was calibrated using a set of globular protein standards (Pharmacia) consisting of thyroglobulin (669 kDa), ferritin (440 kDa), catalase (232 kDa), BSA (67 kDa), and ovalbumin (43 kDa).

Negative staining and EM analysis

CLPs were adhered to a carbon-coated 400-mesh copper grid, blotted to remove excess material, and stained for 2 min with 1% (wt/vol) aqueous solution of uranyl acetate. Images were collected on film with a Hitachi-7000 electron microscope (Hitachi Instruments, CA) operating with an accelerating voltage of 75 kV.

Electron cryo-microscopy

Purified protein for cryo-microscopy was embedded in a thin layer of vitreous ice on glow-discharged holy carbon

films using standard procedure (Dubochet et al., 1988; Hewat et al., 1992). Frozen hydrated specimens were imaged in a Jeol 1200 electron cryo-microscope using a 100-kV electron beam at a magnification of 60 000×. For each specimen area, defocus values of 1 and 2 μm under focus were recorded. Images were recorded on Kodak electron films with 1-s exposure time. Micrographs were developed for 12 min in a Kodak D-19 developer and fixed for 10 min in Kodak fixer.

Analytical centrifugation

Sedimentation velocity experiments were performed using a Beckman Model XL-A centrifuge. The sedimentation velocity experiment was carried out at high speeds using 0.3-cm path length double sector cells with quartz windows. The recombinant protein was diluted to 0.3 mg/ml with 20 mM Tris–HCl (pH 7.5), 50 mM NaCl. Sample volume (400 μl) was centrifuged and radial scan was taken.

Acknowledgments

We are grateful to Peter Prevelige and associates (UAB) for providing us with Analytical Centrifugation facilities, and B.V.V Prasad and J. Bayley (Baylor College of Medicine, USA) for the Cryo-EM facility and their expert assistance. We thank Leigh Millican (UAB, USA) for her technical assistance in electron microscopy. We are indebted to Ian M. Jones (Reading University, UK) for critical proof reading of the manuscript. This work was partly supported by a NIH grant (USA) and the Wellcome Trust (UK).

References

Dryden, K.A., Farsetta, D.L., Wang, G., Keegan, J.M., Fields, B.N. Baker, T.S., Fields, B.N., Nibert, M.L., 1998. Internal/structures containing transcriptase-related proteins in top component particles of mammalian orthoreovirus. Virology 245 (1), 33–46.

Dubochet, J., Adrian, M., Chang, J.J., Homo, J.C., Lepault, J. McDowall, A.W., Schultz, P., 1988. Cryo-electron microscopy of vitrified specimens. Q. Rev. Biophys. 21 (2), 129–228.

Felgner, P.L., Gadek, T.R., Holm, M., Roman, R., Chan, H.W., Wenz, H., Northrop, J.P., Ringold, G.M., Danielson, M., 1987. Lipofectin: a highly efficient, lipid-mediated DNA-transfection procedure. Proc. Natl. Acad. Sci. U.S.A. 84, 7413–7417.

French, T.J., Marshall, J.J., Roy, P., 1990. Assembly of double-shelled, viruslike particles of bluetongue virus by the simultaneous expression of four structural proteins. J. Virol. 64 (12), 5695–5700.

Ghiasi, H., Purdy, M.A., Roy, P., 1985. The complete sequence of bluetongue virus serotype 10 segment 3 and its predicted VP3 polypeptide compared with those of BTV serotype 17. Virus Res. 3 (2), 181–190.

Gilbert, J.M., Greenberg, H.B., 1998. Cleavage of rhesus rotavirus VP4 after arginine 247 is essential for rotavirus-like particle-induced fusion from without. J. Virol. 72 (6), 5323–5327.

Gouet, P., Diprose, J.M., Grimes, J.M., Malby, R., Burroughs, J.N., Zientara, S., Stuart, D.I., Mertens, P.P., 1999. The highly ordered double-stranded RNA genome of bluetongue virus revealed by crystallography. Cell 97 (4), 481–490.

Grimes, J.M., Burroughs, J.N., Gouet, P., Diprose, J.M., Malby, R., Zientara, S., Mertens, P.P.C., Stuart, D.I., 1998. The atomic structure of the bluetongue virus core. Nature 395, 470–478.

Hassan, S.H., Roy, P., 1999. Expression and functional characterization of bluetongue virus VP2 protein: role in cell entry. J. Virol. 73 (12), 9832–9842.

Hewat, E.A., Booth, T.F., Roy, P., 1992. Structure of bluetongue virus particles by cryoelectron microscopy. J. Struct. Biol. 109 (1), 61–69.

Hill, C.L., Booth, T.F., Prasad, B.V.V., Grimes, J.M., Mertens, P.P. Sutton, G.C., Stuart, D.I., 1999. The structure of a cypovirus and the functional organization of dsRNA viruses. Nat. Struct. Biol. 6 (6), 565–568.

Iwata, H., Yamagawa, M., Roy, P., 1992. Evolutionary relationships among the gnat-transmitted orbiviruses that cause African horse sickness, bluetongue, and epizootic hemorrhagic disease as evidenced by their capsid protein sequences. Virology 191 (1), 251–261.

Iwata, H., Yamakawa, M., Roy, P., 1995. International Workshop for the Development of Diagnostic and Preventative Methods by Genetic Engineering for African Horsesickness and Related Orbiviruses, NIAH, Tokyo, Japan.

Kim, J., Zhang, X., Centonze, V.E., Bowman, V.D., Noble, S., Baker, T.S., Nibert, M.L., 2002. The hydrophilic amino-terminal arm of reovirus core shell protein lambda1 is dispensable for particle assembly. J. Virol. 76 (23), 12211–12222.

King, L.A., Possee, R.D., 1992. The Baculovirus Expression System. A Laboratory Guide. Chapman & Hall, London, UK.

Kitts, P.A., Possee, R.D., 1993. A method for producing recombinant baculovirus expression vectors at high frequency. BioTechniques 14, 810–817.

Labbe, M., Baudoux, P., Charpilienne, A., Poncet, D., Cohen, J., 1994. Identification of the nucleic acid binding domain of the rotavirus VP2 protein. J. Gen. Virol. 75 (Pt 12), 3423–3430.

Lawton, J.A., Zeng, C.Q., Mukherjee, S.K., Cohen, J., Estes, M.K., Prasad, B.V.V., 1997. Three-dimensional structural analysis of recombinant rotavirus-like particles with intact and amino-terminal-deleted VP2: implications for the architecture of the VP2 capsid layer. J. Virol. 71 (10), 7353–7360.

Le Blois, H., French, T., Mertens, P.P., Burroughs, J.N., Roy, P., 1992. The expressed VP4 protein of bluetongue virus binds GTP and is the candidate guanylyl transferase of the virus. Virology 189 (2), 757–761.

Limn, C.K., Roy, P., 2003. Intermolecular interactions in a two-layered viral capsid that requires a complex symmetry mismatch. J. Virol. 77 (20), 11114–11124.

Limn, C.-H., Staeuber, N., Monastyrskaya, K., Gouet, P., Roy, P., 2000. Functional dissection of the major structural protein of bluetongue virus: identification of key residues within VP7 essential for capsid assembly. J. Virol. 74 (18), 8658–8669.

Loudon, P.T., Roy, P., 1991. Assembly of five bluetongue virus proteins expressed by recombinant baculoviruses: inclusion of the largest protein VP1 in the core and virus-like proteins. Virology 180 (2), 798–802.

Lu, G., Zhou, Z.H., Baker, M.L., Jakana, J., Cai, D., Wei, X., Chen, S. Gu, X., Chiu, W., 1998. Structure of double-shelled rice dwarf virus. J. Virol. 72 (11), 8541–8549.

Marshall, J.J., Roy, P., 1990. High level expression of the two outer capsid proteins of bluetongue virus serotype 10: their relationship with the neutralization of virus infection. Virus Res. 15 (3), 189–195.

Mellor, P.S., 1990. The replication of bluetongue virus in *Culicoides* vectors. Curr. Top. Microbiol. Immunol. 162, 143–161.

Mertens, P., 1999. Virus Taxonomy. Seventh Report of the International Committee on Taxonomy of Viruses, New York.

Mertens, P.P., Burroughs, J.N., Anderson, J., 1987. Purification and properties of virus particles, infectious subviral particles, and cores of bluetongue virus serotypes 1 and 4. Virology 157 (2), 375–386.

Nason, E., Rothnagel, R., Muknerge, S.K., Kar, A.K., Forzan, M. Prasad, B.V.V., Roy, P., 2004. Interactions between the inner and outer capsids of bluetongue virus. J. Virol. 324, 387–399.

Oldfield, S., Adachi, A., Urakawa, T., Hirasawa, T., Roy, P., 1990. Purification and characterization of the major group-specific core antigen VP7 of bluetongue virus synthesized by a recombinant baculovirus. J. Gen. Virol. 71 (Pt 11), 2649–2656.

Prasad, B.V.V., Yamaguchi, S., Roy, P., 1992. Three-dimensional structure of single-shelled bluetongue virus. J. Virol. 66 (4), 2135–2142.

Prasad, B.V.V., Rothnagel, R., Zeng, C.Q., Jakana, J., Lawton, J.A. Chiu, W., Estes, M.K., 1996. Visualization of ordered genomic RNA and localization of transcriptional complexes in rotavirus. Nature 382 (6590), 471–473.

Purdy, M., Petre, J., Roy, P., 1984. Cloning of the bluetongue virus L3 gene. J. Virol. 51 (3), 754–759.

Reinisch, K.M., Nibert, M.L., Harrison, S.C., 2000. Structure of the reovirus core at 3.6 A resolution. Nature 404 (6781), 960–967.

Roy, P., 1996. Orbivirus structure and assembly. Virology 216 (1), 1–11.

Roy, P., 2001. Orbiviruses and their replication. In: Fields, B.N. (Ed.), 4th ed., Fields' Virology vol. 2. Lippincott-Raven, Philadelphia, pp. 1835–1869.

Sambrook, J., Russell, D.W., 2001. Molecular Cloning: A Laboratory Manual, 3rd ed., Cold Spring Harbor Laboratory Press, Cold Spring Harbor, NY.

Sanger, F., Nicklen, S., Coulson, A.R., 1977. DNA sequencing with chain-terminating inhibitors. Proc. Natl. Acad. Sci. U.S.A. 74, 5463–5467.

Shaw, A.L., Samal, S.K., Subramanian, K., Prasad, B.V.V., 1996. The structure of aquareovirus shows how the different geometries of the two layers of the capsid are reconciled to provide symmetrical interactions and stabilization. Structure 4 (8), 957–967.

Tan, B., Nason, E., Staeuber, N., Jiang, W., Monastryrskaya, K., Roy, P., 2001. RGD tripeptide of bluetongue virus VP7 protein is responsible for core attachment to *Culicoides* cells. J. Virol. 75 (8), 3937–3947.

Tanaka, S., Roy, P., 1994. Identification of domains in bluetongue virus VP3 molecules essential for the assembly of virus cores. J. Virol. 68 (5), 2795–2802.

Tanaka, S., Mikhailov, M., Roy, P., 1995. Synthesis of bluetongue virus chimeric VP3 molecules and their interactions with VP7 protein to assemble into virus core-like particles. Virology 214 (2), 593–601.

Tang, L., Lin, C.S., Krishna, N.K., Yeager, M., Schneemann, A., Johnson, J.E., 2002. Virus-like particles of a fish nodavirus display a capsid subunit domain organization different from that of insect nodaviruses. J. Virol. 76 (12), 6370–6375.

Zeng, C.Q., Estes, M.K., Charpilienne, A., Cohen, J., 1998. The N-terminus of rotavirus VP2 is necessary for encapsidation of VP1 and VP3. J. Virol. 72 (1), 201–208.